

평균FRF를 이용한 장대교량의 동특성

A Dynamic Characterization of Long Span Bridge Using Mean FRF

허 광 희* 최 만 용** 안 병 익***

Heo, Gwang-Hee Choi, Man-Yong An, Byung-Ik

Abstract

구조물의 동특성은 대형구조물을 상시감시 할 수 있는 장점으로 인하여 널리 활용된다. 상시감시를 위해 계측된 랜덤 데이터는 FFT를 통한 구조물의 동적 고유특성을 분석함으로써 이루어진다. 이 과정에서 Input Data와 Response Data사이에서 FFT Analyzer를 통하여 FRF가 측정된다. 특히 랜덤 데이터의 계측은 여건과 환경에 따라 발생하는 Noise로부터 가능한 정확한 FRF를 계측해야만 성공적인 구조물의 고유의 동적특성을 파악하게 된다. 랜덤 데이터에서 발생할 가능성이 높은 입력, 출력 Noise를 동시에 최소화 할 수 있는 새로운 개념의 FRF측정 알고리즘을 제안한다. 이 알고리즘에 의하여 장대형 모형교량으로부터 Modal 실험을 수행하여 계측된 동특성을 FE 해석 결과와 비교 평가하여 유용성을 제시한다.

Keywords : Modal FRF, Dynamic Characterization, Long Span Bridge, FEM, MAC

1. Introduction

U.S. economics supports the vast network of transportation infrastructural facilities in the form of highways, railroads, waterways, transitways, pipelines, etc. The work of the infrastructure is estimated to be around \$2.5 trillion. The U.S. has about 4 million miles of paved roads and highways, and five

hundred seventy five thousand bridges. Statistics from the Federal Highway Department indicate that one third of the bridges[230,000] are functionally and structurally deficient. According to this, two hundred thousand bridges are classified as deficient in need of rehabilitation and require the investment of seventy billion dollars in total.^(1,9) In order to prevent the

* 정회원, 건양대학교, 토목공학과, 교수

** 정회원, 한국표준과학연구원, 시설안전계측연구센터, 책임연구원

*** 건양대학교, 건축공학과, 교수

● 본 논문에 대한 토의를 2000년 3월 31일까지 학회로 보내 주시면 2000년 4월호에 토론결과를 게재하겠습니다.

sudden collapse of the deficient bridges it is necessary to put in place a rigorous bridge monitoring and inspection scheme. While the National Transportation Board recommends that the bridges be inspected every two years, the inspections are still limited only to visual inspection.

What is being proposed in this article is a way of obtaining general information about the relative health of the superstructure of bridges. Subsequently based on the decision-making system, the engineer in charge may decide to carry out more thorough inspection of the actual structure than just visual inspection do, by using a variety of different methods.^(5,-8) One of the methods is the modal test where the test structure is excited by a force. The input and response signals are measured by a Fast Fourier Transform (FFT) analyzer. These time-domain data are then processed and transformed into Frequency Response Functions(FRF). All modal parameters are estimated from these FRFs. Therefore, no matter how good the parameter estimation technique may be, the results will be poor if the FRF is not an accurate representation of the actual structural response. This paper provides the technical background on the different methods available and proposes a new approach for the proper estimation of the FRF.

To solve these problems, most FFT analyzers used the H_1 method to estimate the FRF. In 1982, Mitchell proposed a new improved method called the H_2 method⁽¹⁾. In 1985, Rockin, Crowley and Vold proposed another way of FRF estimation, which investigates an optimum but also practical

way of estimating an accurate FRF for use in experimental modal analysis⁽²⁾. In order to reduce the noise on the input and output signals, the third method of estimating an FRF called the H_{avg} method is suggested as the average or arithmetic means of the H_1 and H_2 methods.

2. FRF Estimation for Random Excitation

Consider the system shown in Fig. 1 which contains a noise both on the input and output. The noise signals $ni(t)$ and $no(t)$ are assumed to be uncorrelated with each other and with $ti(t)$ and $to(t)$.

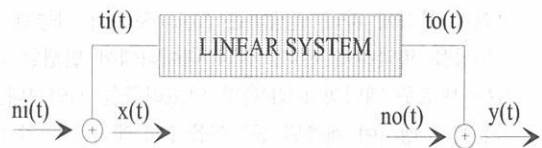


Fig. 1 Linear System with Noise

where

$ni(t)$ and $no(t)$ are the uncorrected noises in the input and output respectively.

$ti(t)$ and $to(t)$ are the true input signals of the measured system and the true output of the system respectively.

$x(t)$ is the input signal measured by the FFT analyzer, which is the same as the true input plus uncorrelated noise.

$y(t)$ is the output signal measured by the FFT analyzer, which is the same as the true output plus uncorrelated noise.

Thus, in the frequency domain, measured output signal is generated as

$$Y(f) = H(f)X(f) + N(f) \quad (1)$$

where $H(f)$ is system function and $X(f)$ and $N(f)$ are input signal and noise signal respectively. Defining the cross spectrum of y relative to x :

$$G_{y,x}(f) = H(f)G_{x,x}(f) + G_{n,x}(f) \quad (2)$$

Two signals are uncorrelated if their cross correlation function is zero. An important theorem developed by Wiener and Hirschman states that the Fourier Transform of the cross correlation function equals to the averaged cross spectral density.^(3,4)

Therefore, we assume that the noise term $G_{n,x}(f)$ averages to zero. The H_1 method is computed by dividing the cross-spectral density of the input to the output by the power spectral density of the input.

$$H_1(f) = \frac{\overline{G_{y,x}(f)}}{\overline{G_{x,x}(f)}} = \frac{\overline{G_{ii,io}(f)}}{\overline{G_{x,x}(f)}} \quad (3)$$

where the bar "—", means the averaged value and G denotes the power spectral density. $\overline{G_{y,x}(f)}$ is the averaged cross spectrum of $y(t)$ relative to $x(t)$. $\overline{G_{x,x}(f)}$ is the averaged auto-spectrum of the input force, $x(t)$. $\overline{G_{ii,io}(f)}$ is the averaged cross-spectral density between the input, $ti(t)$ and the output, $to(t)$. By definition, the true FRF is :

$$H_0(f) = \frac{\overline{G_{ii,io}(f)}}{\overline{G_{ii,ii}(f)}} \quad (4)$$

where $\overline{G_{ii,ii}(f)}$ is the true power spectral density of the input. Following the above system measurement model, one can obtain $G_{x,x} = G_{ii,ii} + G_{ni,ni}$. Substituting the above equation into (4), it yields

$$H_1(f) = \frac{\overline{G_{ii,io}(f)}}{\overline{G_{ii,ii}(f)} + \overline{G_{ni,ni}(f)}} = H_0(f) \left[\frac{1}{1 + \frac{\overline{G_{ni,ni}(f)}}{\overline{G_{ii,ii}(f)}}} \right] \quad (5)$$

According to Eq.(5), $H_1(f)$ approaches to the true FRF, $H_0(f)$, as the averaging count increases, provided that $x(t)$ is noise-free and the noise only $y(t)$ is not correlated with $x(t)$. If $x(t)$ does contain a noise, it will add to the auto-spectrum, so the estimate is low in this case.

The H_1 method is contaminated by the input measurement noise shown in Eq.(5). Therefore, the H_2 method is proposed to define an inverse method for calculating an FRF if the x and y signals are reversed.

$$H_2(f) = \frac{\overline{G_{y,y}(f)}}{\overline{G_{x,y}(f)}} \quad (6)$$

Similarly, the relationship between $H_2(f)$ and the true FRF, $H_0(f)$, is given by

$$H_2(f) = H_0(f) \left[1 + \frac{\overline{G_{no,no}(f)}}{\overline{G_{io,io}(f)}} \right] \quad (7)$$

This inverse FRF estimate, unlike the H_1 method, is not sensitive to the input node.

The H_2 method is a better estimator, especially in the case of random excitation where the input signal is usually low in comparison with the measurement system noise at the resonant frequencies. If the H_1 method is used in this situation, erroneous results will be obtained. On the other hand, the H_2 method remains unaffected. In addition, at resonance, the true output signal is very large compared to the output noise. Thus, the ratio of the output noise to the true input power spectrum, which leads to erroneous estimates when using the H_2 method, is very small when compared to the H_1 method. Therefore, the H_2 method yields an almost perfect estimate of the true H_0 in the region of resonance. However at the anti-resonance, the output power spectrum drops toward the output noise $G_{no,no}(f)$, while the input power spectrum remains high with respect to the input noise power spectrum. Under these conditions, the H_2 method fails to yield acceptable results because of its sensitivity to output noise. In this case, the ratio of $G_{m,m}(f)$ and $G_{no,no}(f)$ is small. Thus, the H_1 method becomes a better estimator of H_0 . The coherence function between two signals $x(t)$ and $y(t)$ is used to detect errors in estimating an FRF.

$$r^2_{y,x}(f) = \frac{H1(f)}{H2(f)} = \frac{\frac{G_{y,x}(f)}{G_{x,x}(f)}}{\frac{G_{y,y}(f)}{G_{x,y}(f)}} = \frac{|G_{y,x}(f)|^2}{G_{x,x}(f) G_{y,y}(f)} \quad (8)$$

where $r^2_{y,x}(f)$ is the coherence function between two signals $x(t)$ and $y(t)$. Clearly, $0 \leq r^2_{y,x}(f) \leq 1$ and $r^2_{y,x}(f)$ equals to 1 only if $H_1(f) = H_2(f)$. According to the discussion above, this condition implies that both $x(t)$ and $y(t)$ are noise-free at frequency (f) . Thus, the coherence function serves as an indicator of data quality, and $1 - r^2_{y,x}(f)$ is the maximum relative error in the estimate of H . The formula above only gives a valid coherence estimate when a sufficient number of independent data blocks have been averaged; until then it is biased high, and for a single block (no averaging) the formula equals to 1 at all frequencies. If the coherence is high (0.95 or greater at the frequencies of interest) based on averaging over several data blocks, then either H_1 or H_2 will produce a valid FRF measurement using a small averaging count, say 5 to 20, depending on the accuracy desired. For modal analysis, high coherence is especially important near resonance frequencies (amplitude peaks in the FRF).

From previous discussions, it can be concluded that the H_1 estimator minimizes the error due to noise on the output but it is very sensitive to noise on the input. This results in an underestimation of the true FRF H_0 around the resonance. Since H_1 is a low bound estimator and H_2 is an upper bound estimator, the true FRF H_0 must lie somewhere in between. This suggests the third method of estimating the FRF as the average or arithmetic means of H_1 and H_2 as follows:

$$H_{avg} = \frac{H_1 + H_2}{2} \quad (9)$$

This estimator is doubly contaminated by input and output noise. Moreover, the high and low estimators tend to correct for one another thus yielding a better estimator of the FRF.

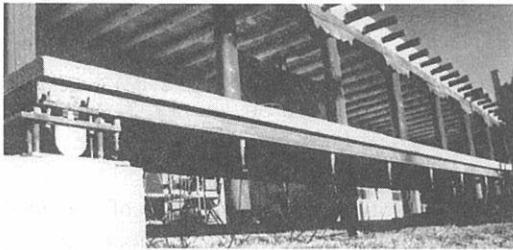


Fig. 2 Description of the Model Bridge

3. Experimental and Numerical Analysis Results of the Bridge

In order to prove the concepts developed in this research it was necessary to perform experiments on an actual structure. A model of a simply supported bridge was built towards this end. A total 528 elements and 359 entities with a 2154 degree of freedom were used to mesh the entire bridge structure as shown in Fig. 3.

The numerical simulation was done by using a normal mode dynamics solver routine in I-DEAS to obtain modal shapes and frequencies. Since FE codes are incapable of modeling structural damping, damping ratios could not be obtained. To compare the numerical model with actual test data, a modal analysis of the model bridge was carried out. The structure was instrumented with accelerometers at 24

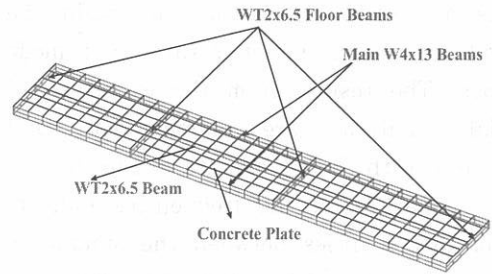


Fig. 3 Meshes of the Bridge with a 2154 Degree of Freedom

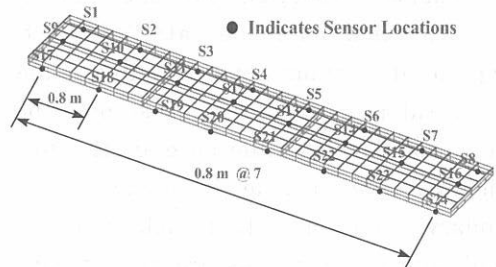


Fig. 4 Accelerometer Locations for Exp. Test for a Model Bridge

locations as shown in Fig. 4. The structure was excited with an impact hammer and the response from the sensors was measured in the form of FRFs (Frequency response Function). The FRF data were then imported into MESScope for modal parameter extraction and mode shape animation. The experimental FRF data was curve fitted by

Table 1 Comparison of Resonant Frequencies (Hz) between Anal. and Exp. Test for a Model Bridge

	Analytical Results	Exp. Results	
Mode #	Freq. (Hz)	Freq. (Hz)	Dam. (%)
Mode 1	11.160	8.440	0.200
Mode 2	21.140	22.290	0.130
Mode 3	28.660	29.000	0.510
Mode 4	51.760	51.440	3.260
Mode 5	57.340	55.170	4.550
Mode 6	71.480	67.070	2.750

using a method of residues to obtain the modal frequency, damping ratio and mode shapes. The results from the experimental modal analysis are summarized and compared with the FE results in Fig. 5.

A comparison of the frequencies indicate minor discrepancies between the simulation and test results. The significant difference in frequency is only restricted to the first mode. In a situation where differences between simulated and experimental results are observed through all the modes, the difference can be attributed to inappropriate assumptions of material and geometrical properties. The most plausible explanation for the difference in the first mode may lie in the modeling of the boundary conditions. It is felt that the actual support conditions are more flexible than assumed at the modeling stage. A more objective way of comparing the numerical results with the experimental

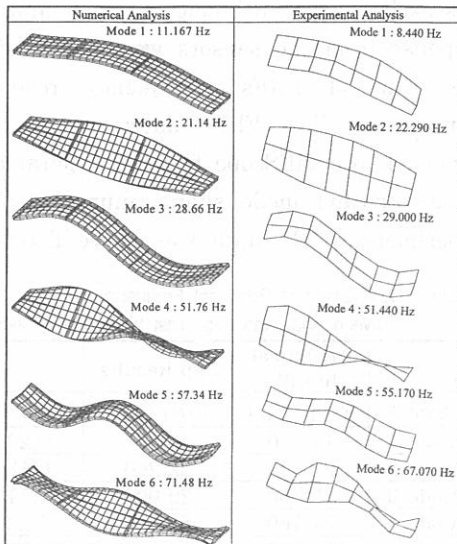


Fig. 5 Comparison of Mode Shapes of a Model Bridge

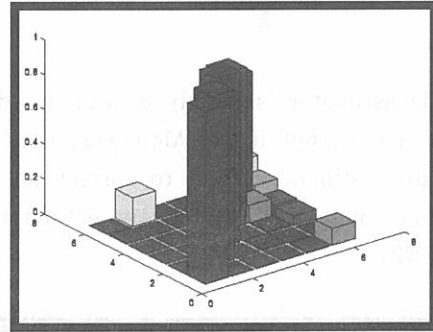


Fig. 6 Comparison of Mode Shapes (MAC) Between Anal. and Exp. Results for a Numerically Simulated Long Span Bridge

results involves the comparison of the mode shapes obtained by each method. This is done through a process called MAC as shown in Fig. 6.

4. Conclusions

The authors have derived an averaged FRF technique for the dynamic characterization of long span type bridges. In this proposed method the emphasis is to apply it to long span bridges. The numerical analysis and experimental test of the bridge using the proposed method are carried out. The FEM analysis of the bridge provided a fairly good estimate of the actual modal parameters of the bridge. These experimental results indicate that the modes beyond the first four modes are characterized by very high damping ratios, making it harder to identify the higher modes experimentally. The results show that the algorithm is good enough to use for the purpose of the health monitoring of long span bridges.

References

1. Mitchell, L.D., "Improved Methods for the Fast Fourier Transform (FFT) Calculation of the Frequency Response Function", ASME Journal of Mechanical Design, Vol. 104, 1982, pp. 277-279
2. Rocklin, G. T., Crowley, John, and Vold, Havard , "A Comparison of H1, H2, Hv Frequency Response Functions", IMAC Conference Proceedings, Vol. 1, 1985, pp. 272-278
3. Vold, Havard and Rockline, G. Thomas, "The Numerical Implementation of a Multi-Input Modal Estimation Method for Mini-Computers," Proceedings of the 1st International Modal Analysis Conference, Nov. 8-10, 1982, Holiday Inn, International Drive Orlando, Florida, pp. 542-548
4. Ewins, D.J., "Modal Testing: Theory and Practice", Research Studies Press LTD., John Wiley & Son Inc, 1994.
5. Gwanghee Heo, "An Automated Health Monitoring System for Large Civil Structural Systems," Ph.D. Dissertation, University of New Mexico, 1996.
6. 허 광희, 최만용, "계측된 구조물의 동적인자에 의한 손상검출기법," 『한국구조물진단학회』, 제2권, 제4호, 1998.
7. M. L. Wang, Gwanghee Heo, D. Satpathi, "Dynamic characterization of a long span bridge: a finite element based approach," Soil Dynamic and Earthquake Engineering, 16, 1997.
8. G. Heo, M. L. Wang, D. Satpathi, "Optimal transducer placement for health monitoring of long span bridge," Soil Dynamic and Earthquake Engineering, 16, 1997
9. Nazarian, Sheil and Olson, Larry D., "Nondestructive Evaluation of Aging Structures and Dams," SPIE Vol. 2457, 1995.

(접수일자 : 1999. 10. 28)